www.acsnano.org

Quantifying Order during Field-Driven Alignment of Colloidal Semiconductor Nanorods

Rivi J. Ratnaweera, Freddy A. Rodríguez Ortiz, Nicholas J. Gripp, and Matthew T. Sheldon*



Downloaded via TEXAS A&M UNIV COLG STATION on July 27, 2022 at 13:28:40 (UTC). See https://pubs.acs.org/sharingguidelines for options on how to legitimately share published articles.

Cite This: ACS Nano 2022, 16, 3834-3842



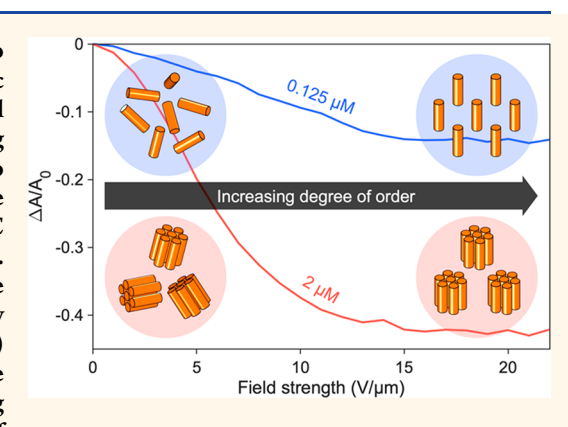
ACCESS

III Metrics & More

Article Recommendations

s Supporting Information

ABSTRACT: Aligning large populations of colloidal nanorods (NRs) into ordered assemblies provides a strategy for engineering macroscopic functional materials with strong optical anisotropy. The bulk optical properties of such systems depend not only on the individual NR building blocks but also on their meso- and macroscale ordering, in addition to more complex interparticle coupling effects. Here, we investigate the dynamic alignment of colloidal CdSe/CdS NRs in the presence of AC electric fields by measuring concurrent changes in optical transmission. Our work identifies two distinct scales of interaction that give rise to the field-driven optical response: (1) the spontaneous mesoscale self-assembly of colloidal NRs into structures with increased optical anisotropy and (2) the macroscopic ordering of NR assemblies along the direction of the applied AC field. By modeling the alignment of NR ensembles using directional statistics, we experimentally quantify the maximum degree of



order in terms of the average deviation angle relative to the field axis. Results show a consistent improvement in alignment as a function of NR concentration—with a minimum average deviation of 36.2°—indicating that mesoscale assembly helps facilitate field-driven alignment of colloidal NRs.

KEYWORDS: colloidal nanorod, AC field alignment, nanorod assembly, optical anisotropy, electro-optic

olloidal semiconductor nanorods (SC NRs) have been widely studied as potential building blocks for optoelectronic devices¹⁻⁷ due to their strong optical anisotropy, tunable band-edge emission, and near-unity photoluminescence (PL) quantum yield.⁸⁻¹¹ These one-dimensional nanocrystals exhibit stronger quantum confinement¹² perpendicular to their long axes, which modifies the spatial distribution of photoexcited charge carries, giving rise to pronounced optical anisotropy in the form of linearly polarized absorption and emission of light (see Figure 1).^{9,11} Recent advances in nanoparticle synthesis have further enabled precise control of size, composition, and morphology, affording tailored spectral- and angle-dependent absorption and emission patterns in these and related nanocrystalline materials.^{13,14}

The distinctive optical properties of individual NRs can be exploited at the macroscopic scale by assembling large populations of NRs into ordered superstructures. For instance, several studies have highlighted the promise of aligned anisotropic luminophores for application in luminescent solar concentrators ^{4,5,15} and liquid crystal displays. ^{16,17} The ensemble properties of NR assemblies are determined not

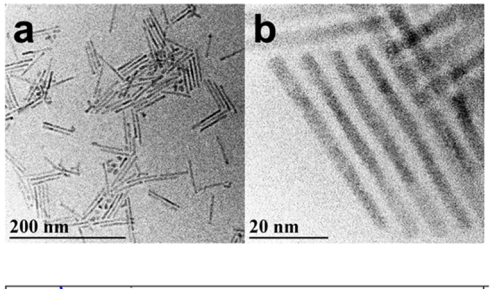
only by the individual NR building blocks but also by their meso- and macroscale ordering, as well as more complex interparticle coupling effects. Numerous techniques for collective alignment of NRs have been explored, and they can be broadly classified into two approaches: (1) taking advantage of the self-assembly of colloidal NRs into superlattices and (2) applying external stimuli such as mechanical rubbing, selectric fields, $^{26-29}$ or magnetic fields to promote orientation along a preferred axis.

To date, there has been significant progress studying the alignment of colloidal SC NRs in solution by AC electric fields as a strategy for producing functional materials with strong electro-optic modulation of optical anisotropy, typically in the 0.5–10 kHz frequency regime. ^{27,31} The underlying mechanism

Received: September 26, 2021 Accepted: February 16, 2022 Published: February 21, 2022







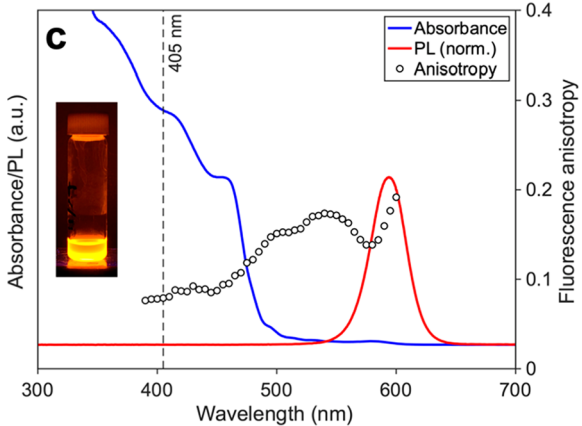


Figure 1. (a,b) Transmission electron micrographs of CdSe/CdS nanorods. (c) Absorbance, photoluminescence (normalized), and ensemble fluorescence anisotropy spectra (inset: PL emission of colloidal CdSe/CdS NRs under UV illumination).

is based on torquing the electrostatic dipole moment in NRs—largest along the long axis—by means of an externally applied electric field, leading to collective alignment of NRs parallel to the field direction.²⁷ Previous reports have attributed the electrostatic dipole moment in cadmium chalcogenide NRs to an intrinsic permanent dipole moment arising from their noncentrosymmetric wurtzite crystal structure.³² Additionally, in the presence of an external electric field, induced dipole moments may also contribute to the overall electrostatic dipole moment along the long axis.²⁷

The alternating magnitude of an applied AC field causes the NR ensemble to oscillate between aligned and randomly oriented configurations. Since NRs preferentially absorb light with polarization that is parallel to their long axes, switching between aligned and random configurations can give rise to a periodic change in absorbance, ^{27,31,33} up to a relative change of 53%, as demonstrated by Mohammadimasoudi et al.²⁷ In a typical geometry (see Figure 2a), where the sample is excited with light that is polarized perpendicular to the electric field, the absorbance of the sample decreases with an increasing degree of alignment. This manifestation of the AC field-driven ordering in the time-dependent absorbance signal has been used to quantify the alignment in a NR ensemble, with the highest possible degree of order targeted as the most beneficial for optoelectronic applications.

Recent studies have reported partial³¹ and quasi-complete²⁷ alignment of SC NRs in the presence of AC electric fields based on the field-induced relative change in absorbance. These reports, however, interpret data under the assumption that individual NRs are isolated in solution, and that the ensemble response can be attributed to the collective behavior of the individual isolated NRs.

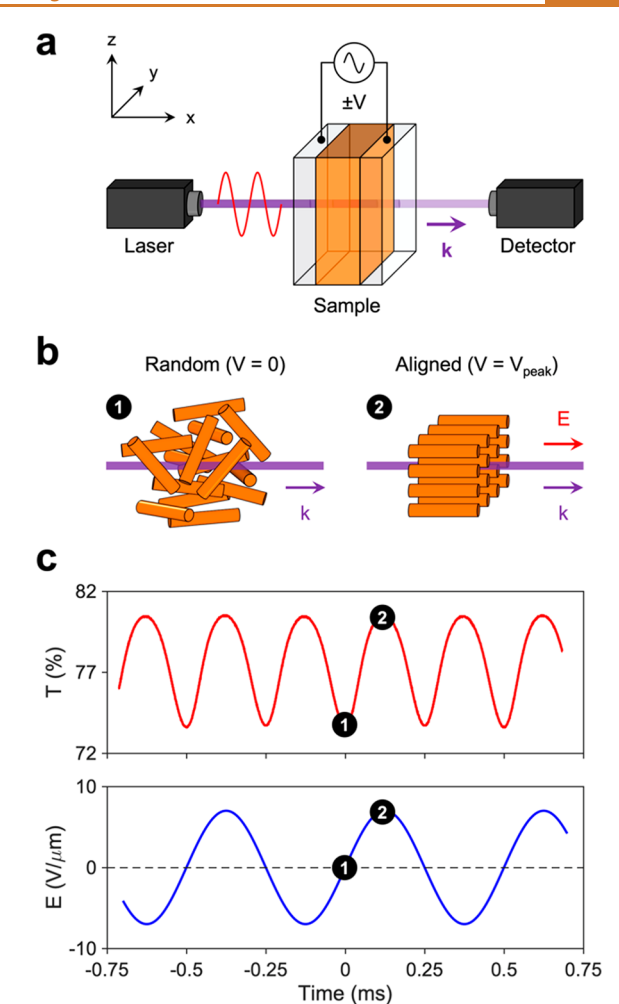


Figure 2. (a) Schematic representation of the experimental setup. (b) Alignment of NRs in the presence of an AC field when the magnitude of the applied voltage is equal to (1) zero and (2) the peak voltage. (c) Variation of applied field strength (bottom) and concurrent percent optical transmittance (top) as a function of time for a 2 μ M colloidal dispersion of CdSe/CdS NRs in the presence of a 2 kHz, \pm 7 V/ μ m AC electric field.

Yet, growing evidence suggests that more complex interactions may be involved in the dynamic alignment of NRs. For example, colloidal SC NRs have been shown to spontaneously self-assemble into aggregated, microscale bundles in solution at concentrations as low as 1 μ M. Moreover, several previous studies indicate that the energetics associated with aligning individual NRs in an externally applied field—up to field strengths that cause dielectric breakdown of the solvent system—minimally counteract the thermal energy of free rotation, if at all. ^{27,31} Instead, synergistic effects between NRs may be partially responsible for the observed alignment. In this alternative picture, bundles or aggregates of NRs in solution are more polarizable by externally applied electrostatic fields compared to individual NRs, thereby enabling the pronounced field-driven response that is observed.

Solution-phase self-assembly into bundles is also likely to modify the absorption anisotropy and other optical properties of colloidal NRs. For example, Pietra et al. observed increased linear dichroism when solutions of self-assembled NR bundles were placed in strong magnetic fields.³⁰ The spontaneous aggregation of NRs into bundles—even in the absence of any

external fields—complicates interpretations of ordering during optical measurements. Thus, ascertaining the optical anisotropy and related properties of the predominant NR species, i.e., isolated NRs or NR bundles, is critical for accurately quantifying the degree of field-driven ordering.

In this study, we investigate the alignment of colloidal CdSe/CdS core/shell NRs by probing the AC field-driven optical response. A statistical model based on a third-order von Mises—Fisher distribution, 34 i.e., a normal distribution describing three-dimensional vector orientations, is used in conjunction with ensemble fluorescence anisotropy measurements to determine the average NR orientation relative to the direction of the applied field. We examine how varying the concentration of NRs impacts their electro-optic response and ensemble anisotropy to gain further insight into the spontaneous mesoscale self-assembly.

An important insight from our study is the different scales of interaction that give rise to the macroscopic optical response. We see clear evidence for the aggregation or self-assembly of NRs in solution manifest as increased optical anisotropy compared to that of isolated NRs, as well as features consistent with aggregate formation in small-angle X-ray scattering (SAXS) studies. Further, we observe that these self-assembled aggregates are more readily aligned by an external electrostatic field, giving rise to a greater overall orientational order as well as stronger field-driven modulation of absorbance. Our approach highlights the contrasting electrokinetic behavior of individual versus aggregated NRs and allows for quantitative determination of the degree of order using an optical analysis that accounts for these mesoscale self-assembly effects as well as the macroscopic field-driven behavior of the entire ensemble.

RESULTS AND DISCUSSION

Optical Response of Colloidal CdSe/CdS NRs. The field-driven alignment of colloidal CdSe/CdS core/shell NRs was investigated by measuring their time-dependent optical response in the presence of alternating current (AC) electric fields. Dodecane-based dispersions of CdSe/CdS NRs were loaded into 50 μ m thick sample cells (Figure S5 in Supporting Information) and exposed to uniform AC fields, as depicted in Figure 2a. In order to avoid accumulation of NRs at the electrodes, a sufficiently high AC frequency (2 kHz) was chosen, ensuring that the dynamic alignment of NRs occurs at a faster time scale compared to the cell transit time of any charged species.²⁷ Concurrently, the time-dependent optical transmittance of the samples was monitored at 405 nm using a collimated light source and a photoreceiver (see Figure 2a). The CdSe/CdS NRs used in this study were synthesized following a procedure³⁵ described in literature, and the material properties of the samples were characterized using transmission electron microscopy (TEM), powder X-ray diffraction (XRD), and UV-vis spectroscopy (Figure 1), in addition to optical anisotropy measurements detailed below.

Figure 2c shows the transient optical response of a 2 μ M dispersion of NRs in the presence of a ± 7 V/ μ m AC field. The transmittance of the sample fluctuates in response to the periodic alignment and relaxation via rotational diffusion of NRs. At zero field strength (1), the NRs are randomly oriented in solution (see Figure 2b), and the transmittance is at a minimum (maximum absorbance). However, as the field strength is gradually increased, the NRs begin to align parallel to the field direction—and perpendicular to the polarization of

the incident laser beam—resulting in an overall decrease in absorbance and, consequently, an increase in transmittance. At peak field strength (2), the transmittance reaches a maximum, indicative of the system having reached a maximum degree of alignment for that magnitude of applied field. The rapid alignment and relaxation of NRs which occur at a millisecond time scale can be perceived by the naked eye as a time-averaged increase in optical transmission (see Figure 3b).

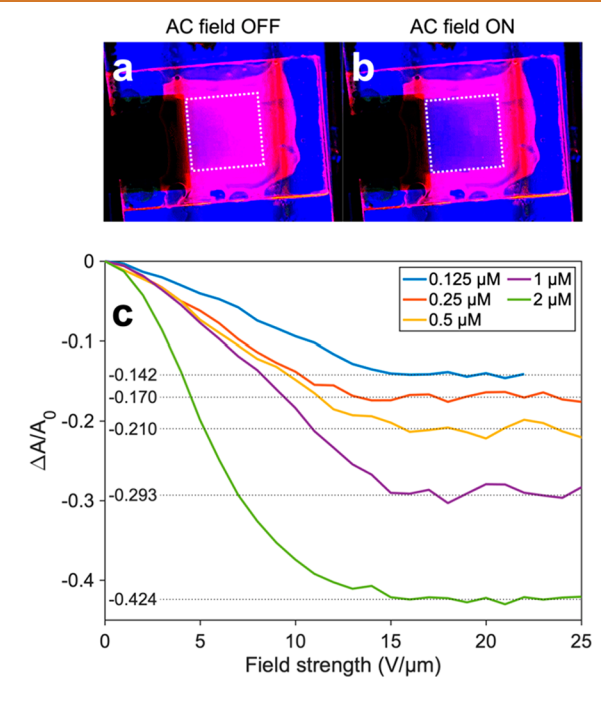


Figure 3. Overhead view of a 2 μ M dispersion of CdSe/CdS nanorods under UV illumination in the presence of (a) no applied field and (b) a ± 24 V/ μ m AC field. (c) Variation of $\Delta A/A_0$ as a function of field strength measured for samples with different NR concentration.

The magnitude of the periodic absorbance shift is correlated with the degree of alignment in the NR ensemble: higher degrees of order result in larger shifts in absorbance. The relative change in absorbance ($\Delta A/A_0$) has been proposed as a quantitative measure of ensemble alignment that is independent of external factors such as cell thickness, NR concentration or laser power (eq 1).²⁷

$$\frac{\Delta A}{A_0} = \frac{A_{\text{peak}} - A_0}{A_0} \tag{1}$$

describes $\Delta A/A_0$ in terms of the absorbance at peak voltage (A_{peak}) and the absorbance when no external field is applied (A_0) .

The variation of $\Delta A/A_0$ was recorded as a function of field strength for five different NR concentrations (Figure 3c). In each case, the magnitude of $\Delta A/A_0$ was found to increase with field strength and saturate at approximately 15 V/ μ m, showing excellent agreement with previous studies. However, the limiting optical response exhibits a strong dependence on NR concentration: $\Delta A/A_0$ saturates at more negative values for samples with higher NR concentration, suggesting an overall improvement in ordering. We believe that the trend in $\Delta A/A_0$ can be attributed to interparticle interactions that facilitate alignment, in particular, the spontaneous self-assembly of

colloidal NRs into rafts or bundles, an effect that has been observed in similar colloidal systems. Increasing the NR concentration likely enhances the free-energy driving force for the formation of aggregates, resulting in an augmented electro-optic response. Following the work of Pietra et al., we performed SAXS measurements to verify the existence of said aggregates (see Figure S9 in Supporting Information). Our results show the emergence of a broad peak centered around $\sim\!0.7~{\rm nm}^{-1}$ as the NR concentration is increased, suggesting the formation of aggregates in solution.

It is important to note that the field-induced optical response of NRs depends not only on their ordering in solution but also on the ensemble optical anisotropy of the colloidal species. For example, given the same degree of order, NRs with a more ideal dipolar absorption pattern would produce a larger shift in absorbance compared to NRs with a more isotropic absorption pattern. Therefore, quantitatively analyzing the absorption anisotropy of the colloidal species is crucial for accurate determination of the overall ordering.

Ensemble Optical Anisotropy Measurements. The optical anisotropy of SC NRs is typically determined either by measuring the polarization-dependent PL emission from individual NRs^{9,11} or by measuring the ensemble fluorescence anisotropy of samples in solution. Here, we employ the latter approach as it samples the entire NR ensemble and preserves any superstructures that may form in solution. In a typical experiment, a random ensemble of NRs is excited by a vertically polarized source that selectively excites transition dipoles based on the projection of these dipoles parallel to the polarization axis of excitation. here dipoles parallel to the polarization axis of excitation. The PL emission from excited NRs is measured at an angle of 90° relative to the excitation beam, through a vertical or horizontal polarizing filter (see Figure S6 in Supporting Information). The ensemble fluorescence anisotropy (r) is defined according to eq 2:

$$r = \frac{I_{\parallel} - I_{\perp}}{I_{\parallel} + 2I_{\perp}} \tag{2}$$

where I_{\parallel} and I_{\perp} are the vertically and horizontally polarized emission intensities, respectively. ^{36,37}

The anisotropy of a random ensemble of emitters can, in theory, range between -0.2 and 0.4 depending on (1) the intrinsic dipole moment of the optical transition and (2) depolarization due to mismatch of excitation and emission dipole moments-typically caused by rotational diffusion between the excitation and emission events. The latter effect, while prominent in dichroic dyes, 36,37 can be regarded as negligible in SC NRs as the rotational diffusion rate (>1 μ s), even in low-viscosity solvents at room temperature, is significantly slower compared to the fluorescence lifetime (10-50 ns). 10 Dilute solutions of CdSe/CdS NRs have been experimentally shown to exhibit a peak anisotropy of ~0.2 for near band-edge excitation and consistently lower values (~0.1) at higher energy excitation (Figure 1c). 9-11 Samples with no optical anisotropy show values of r = 0, whereas ensembles of randomly oriented ideal dipoles show r = 0.4.^{36,3}

While conventional fluorescence anisotropy offers insight into the overall dipole nature of the collective absorption—reemission process, by itself, it is unable to independently determine the absorption and emission anisotropies. We have developed an alternative technique that complements conventional fluorescence anisotropy measurements, facilitating the independent characterization of the absorption dipole. Our

method involves the excitation of a colloidal sample with circular-polarized light and the collection of PL emission at an angle of 90° relative to the excitation axis. The ensemble anisotropy in this case (r_{\odot}) is calculated using the same expression as before (eq 2). However, the contrasting photoselection of transition dipoles arising from the distinct polarization mode results in an altered dynamic range for anisotropy values. Random ensembles of isotropic (r=0) and ideal dipole (r=0.4) emitters would yield values of $r_{\odot}=0$ and $r_{\odot}=0.25$, respectively. Taken together, the values of r and r_{\odot} define a system of equations that can be solved for the absorption anisotropy and emission anisotropy independently (see Supporting Information for complete derivation of this method).

Figure 4a shows the conventional (solid blue markers) and circular-polarized (solid green markers) ensemble anisotropy

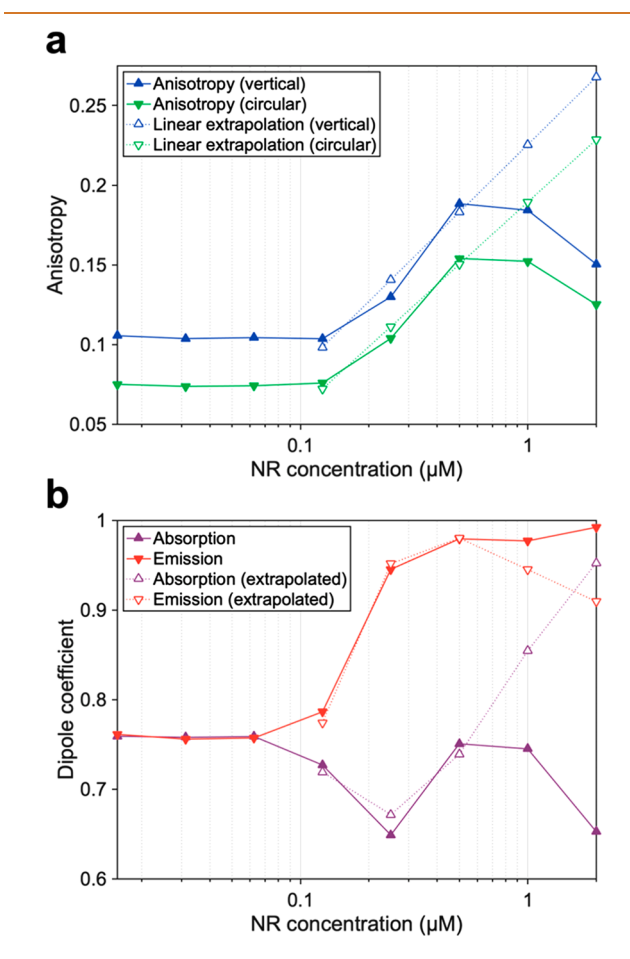


Figure 4. Variation of (a) ensemble fluorescence anisotropy of CdSe/CdS NRs at 405 nm and (b) corresponding absorption and emission dipole coefficients plotted against NR concentration.

of CdSe/CdS NRs recorded as a function of NR concentration. The strong spectral dependence of anisotropy in SC NRs (Figure 1c) requires that the ensemble anisotropy measurements be carried out at the same excitation wavelength (405 nm) as in the $\Delta A/A_0$ measurements. As evident from both trends, the variation of ensemble anisotropy reveals a strong dependence on NR concentration, which we interpret as three regimes of contrasting behavior.

In the dilute regime ($\leq 0.125 \ \mu\text{M}$), the anisotropy remains consistent and comparable to previously reported values, ⁹⁻¹¹

suggesting that NRs exist as individual isolated particles in solution. However, at intermediate concentrations (0.125–0.5 μ M), both anisotropy values increase with increasing NR concentration. We attribute this positive correlation to the selfassembly of NRs leading to the formation of mesoscale structures that have more ideal transition dipoles compared to individual NRs. This hypothesis concurs with proposed colloidal-phase NR assemblies³⁰ in which NRs are aggregated in a side-by-side manner so that their long axes are coaligned. The decrease in anisotropy observed at higher concentrations (>0.5 μ M) can be attributed to multiple scattering and/or multiple reabsorption and re-emission events, typical artifacts in ensemble anisotropy measurements when incident photons interact with more than one species before reaching the detector.³⁷ In order to estimate the vertical- and circularpolarized anisotropies of the NR colloids independent of these artifacts intrinsic to the measurement, we have extrapolated the positive trends observed in the 0.125–0.5 μ M regime (hollow markers). This extrapolation aids further analysis provided below, though we acknowledge that this approximation is not a rigorous assessment of the true anisotropy but is, instead, a rough estimate pertaining to the limiting case where the anisotropy values continue to increase with increasing NR concentration. For the sake of simplicity, linear trendlines (on a logarithmic x-axis) were used to extrapolate the data in the high-concentration regime.

While NRs exhibit strong linearly polarized absorption and emission, their optical behavior deviates from those of ideal dipoles, in part, due to features of their band structure. Previous studies have treated this nonideal optical behavior by considering a linear combination of isotropic and dipole character. 4,5 Using a similar approach, we have derived (see Supporting Information) theoretical expressions for verticaland circular-polarized ensemble anisotropy of NRs, where the dipole nature of absorption and emission is defined using the linear interpolation parameters χ_a and χ_e , respectively. These parameters are mutually independent and can each range from 0 to 1, with 0 representing isotropic absorption/emission and 1 representing ideal dipole absorption/emission. As detailed in the Supporting Information, the correlation between the ensemble anisotropies $(r \text{ and } r_{\uparrow})$ and the two dipole coefficients can be solved as a system of simultaneous equations to independently determine χ_a and χ_e .

Figure 4b depicts the concentration-dependent trends of χ_a (purple markers) and χ_e (red markers), each calculated using measured (solid markers) as well as extrapolated (hollow markers) ensemble anisotropy data. In the dilute regime ($\leq 0.125~\mu\text{M}$), the two coefficients remain constant (~ 0.76) and approximately equal to one another. However, as the solutions become more concentrated—and presumably, more aggregated— χ_e begins to dominate, approaching near-unity at the highest concentration. The variation of χ_a follows a less conclusive trend: the calculated values decrease on average with increasing NR concentration, although the extrapolated values show a clear increase.

Theoretical Model. In order to translate the measured $\Delta A/A_0$ and ensemble anisotropy data into a quantitative measure of the orientational order, we developed an expression that predicts $\Delta A/A_0$ in terms of (1) the intrinsic absorption anisotropy of the colloidal species and (2) the degree of field-driven macroscale ordering. The absorbing species could be either an individual isolated NR or a self-assembled NR

bundle. Our model simply assumes an arbitrary absorber/emitter with an intrinsic optical dipole.

The collective ordering of absorbers along the axis of the driving AC field is modeled using a third-order von Mises—Fisher distribution.³⁴ The probability (f_p) of an absorber being oriented along an arbitrary direction (r) can be expressed according to eq 3:

$$f_{p}(\mathbf{r};\boldsymbol{\mu},\kappa) = \frac{\kappa}{2\pi(e^{\kappa} - e^{-\kappa})} \exp(\kappa \boldsymbol{\mu}^{T} \mathbf{r})$$
(3)

where the parameters μ and κ represent, respectively, the direction of the externally applied field and the so-called focus factor. The parameter κ can take on any value from 0 (randomly oriented ensemble of emitters) to infinity (perfectly aligned ensemble of emitters) and is directly correlated with the average deviation angle $(\overline{\theta})$ of the emitters relative to the unit vector μ (see Figure S10 in Supporting Information).

According to Beer's law, the absorbance (A) of a colloidal dispersion of nanoparticles can be expressed as shown in eq 4:

$$A = \left(\frac{N_{\rm A}}{\ln 10}\right) \cdot \overline{\sigma} \cdot c \cdot l \tag{4}$$

where *c* is the concentration, *l* is the path length, and $\overline{\sigma}$ is the average attenuation cross section.³⁸

This formalism can be adapted to calculate the absorbance of an ordered ensemble of NRs or NR bundles considering the angle-dependent absorption cross section of individual absorbers. If each particle behaves as an ideal dipole absorber, the attenuation cross section (σ) of an arbitrarily oriented absorber excited by linearly polarized light (along the X-Z plane in Figure 5) is related to its zenith (θ) and azimuth (φ) angles according to eq 5:

$$\sigma(\theta, \varphi) = k \sin^2 \theta \cos^2 \varphi \tag{5}$$

where k represents a proportionality constant.

The average attenuation cross section of an ensemble $(\overline{\sigma})$ can be calculated according to eq 6:

$$\overline{\sigma}(\kappa) = \int_0^{2\pi} \int_0^{\pi} f_{\rm p}(\theta, \varphi) \sigma(\theta, \varphi) \mathrm{d}\theta \mathrm{d}\varphi \tag{6}$$

by integrating the single-particle attenuation cross section (σ) weighted by the normalized probability density of orientations $(f_{\rm p})$. The angles θ and φ represent the zenith and azimuth angles of an arbitrary absorber, respectively.

Combining eq 4 and eq 6 yields eq 7:

$$A = \left(\frac{N_{\rm A}cl}{\ln 10}\right) \int_0^{2\pi} \int_0^{\pi} f_{\rm p}(\theta, \varphi) \sigma(\theta, \varphi) d\theta d\varphi \tag{7}$$

which describes the ensemble absorbance (A) in terms of concentration (c), path length (l), and single-particle cross section (σ).

Substituting for absorbance in eq 1 negates the dependence on concentration and path length, resulting in eq 8:

$$\frac{\Delta A}{A_0} = \frac{\overline{\sigma}(\kappa) - \overline{\sigma}(\kappa = 0)}{\overline{\sigma}(\kappa = 0)} \tag{8}$$

which can be used to calculate the relative change in absorbance $(\Delta A/A_0)$ as a function of the focus factor (κ) .

The predicted $\Delta A/A_0$ decreases with increasing order and saturates at a minimum value as the system approaches complete alignment $(\kappa \to \infty)$, i.e., when the transition dipoles align perpendicular to the polarization axis of the excitation.

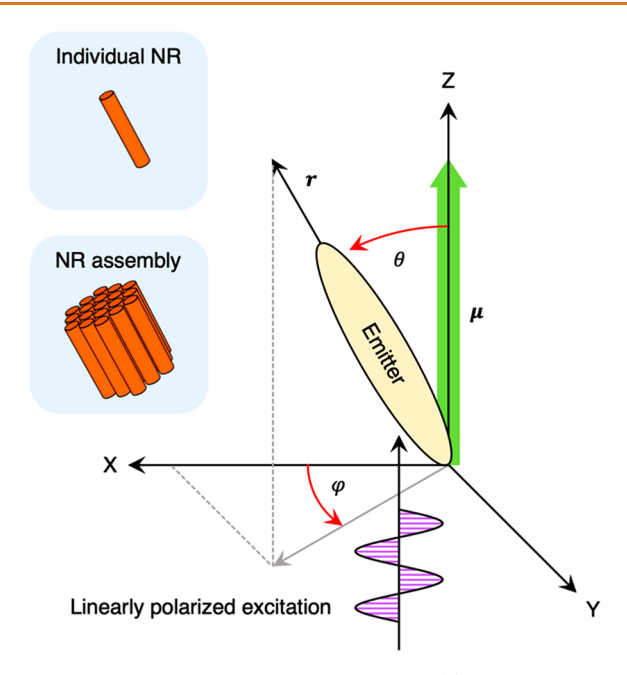


Figure 5. Orientation of an arbitrary emitter (r) and applied field direction (μ) defined in terms of zenith (θ) and azimuth (φ) angles based on a Cartesian coordinate system. The axis of optical excitation polarization lies along the X-Z plane. The emitter could be an individual isolated NR or a self-assembled NR bundle (inset).

For an ensemble of ideal dipoles, this limiting value of $\Delta A/A_0$ would be equal to -1 due to the complete absence of an absorption cross section when fully aligned $(\overline{\sigma}(\infty) = 0)$. In the case of real NRs, however, the correlation between κ and $\Delta A/A_0$ is less trivial as their optical behavior deviates from that of ideal dipoles.

In order to approximate the angle-dependent absorption cross section of a real NR, we modify the expression for the single-particle absorption cross section of an ideal dipole (eq 5) according to eq 9:

$$\sigma(\theta) = k[\chi_{a} \sin^{2} \theta \cos^{2} \varphi + (1 - \chi_{a})]$$
(9)

where the aforementioned parameter, χ_a (0 $\leq \chi_a \leq 1$), describes the dipole character of an individual absorber, i.e., how closely its absorption resembles that of an ideal dipole ($\chi_a = 1$) or an isotropic emitter ($\chi_a = 0$).

Using the correlation between $\Delta A/A_0$ and κ (eq 8), we have calculated the degree of order in each sample in terms of the average $(\overline{\theta})$ and statistical standard deviation (SD) of the deviation angle of emitters relative to the field axis (θ) . Table 1 summarizes the limiting $\Delta A/A_0$, vertical- and circular-polarized ensemble anisotropy and maximum degree of order for each

sample. For NR concentrations above 0.5 μ M, we have also included estimated values of $\overline{\theta}$ and SD obtained using extrapolated ensemble anisotropy data (hollow markers in Figure 4a).

In the regime where anisotropy measurements are free of scattering artifacts (\leq 0.5 μ M), the average deviation angle decreases with increasing NR concentration, suggesting that macroscopic field-driven ordering improves as the degree of mesoscale self-assembly is increased. That is, it appears that NR aggregates align more easily and order more completely compared to individual isolated NRs.

At higher NR concentrations (>0.5 μ M), the ensemble anisotropy values—and thereby, the dipole coefficients—are affected by scattering and/or reabsorption of fluorescent emission. While we have taken measures to reduce the impact of these artifacts, specifically, by using a narrow cuvette with a shorter fluorescence path length (~2 mm), we understand that these artifacts may still influence the final analysis. To correct for this potential complication, we have also calculated average deviation angles using extrapolated ensemble anisotropy data. As summarized in the last two columns of Table 1, this correction appears to lower the degree of ordering above 0.5 μ M, compared to the respective fitted values. Nevertheless, the extrapolated degree of order continues to increase as a function of NR concentration.

Finally, we note that we have also performed studies to promote the formation of NR bundles by adding a varying amount of antisolvent that decreases colloidal stability (see Figure S8 in Supporting Information). Our results are consistent with the dependence on NR concentration discussed above: the ensemble anisotropy increases with increasing concentration of antisolvent (decreasing colloidal stability).

Overall, these results support our hypothesis that the electro-optic response arises due to separate contributions from (1) the optical anisotropy of mesoscale NR assemblies that form in the absence of applied fields and (2) macroscopic ordering imposed by the electrostatic forces of the driving AC field. The greater magnitude of $\Delta A/A_0$ at higher NR concentrations is attributed both to an increase in the absorption anisotropy of the emitting species, i.e., the formation of NR bundles, as well as a greater susceptibility of these bundles to field-driven ordering. While the magnitude of the experimentally measured $\Delta A/A_0$ in our study is comparable with previous reports,²⁷ our analysis indicates a significantly lower degree of maximum NR alignment. The disparity lies in the treatment of individual absorbers: instead of assuming colloidal NRs to be individual isolated particles, we treat them as aggregated bundles with varying degrees of characteristic concentration-dependent optical anisotropy.

Table 1. Summary of Limiting $\Delta A/A_0$, Ensemble Fluorescence Anisotropy, and Average Deviation Angle at Maximum Alignment

		anisotropy (vertical)		anisotropy (circular)		average dev. angle, $\overline{\theta} \pm \mathrm{SD} \; (\mathrm{deg})$	
NR concn (µM)	limiting $\Delta A/A_0$	measured	extrapolated	measured	extrapolated	fitted (eq 8)	extrapolated
0.125	-0.142	0.1036	0.0982	0.0758	0.0721	50.9 ± 28.8	50.6 ± 28.7
0.25	-0.170	0.1299	0.1406	0.1038	0.1112	44.7 ± 25.3	45.6 ± 25.8
0.5	-0.210	0.1884	0.1830	0.1540	0.1503	44.3 ± 25.0	43.8 ± 24.8
1	-0.293	0.1843	0.2254	0.1522	0.1894	36.9 ± 20.5	41.0 ± 23.1
2	-0.424	0.1505	0.2678	0.1251	0.2285	21.4 ± 11.4	36.2 ± 20.1

CONCLUSIONS

We have demonstrated AC field-driven mechanical alignment of colloidal CdSe/CdS NRs by measuring concurrent changes in optical transmission. Our work identifies two distinct scales of interaction that give rise to the macroscopic optical response: (1) the spontaneous mesoscale self-assembly of colloidal NRs into bundles with optical anisotropy greater than that of ensembles of individual NRs and (2) the macroscale ordering of NR assemblies along the direction of the applied driving field. Ensemble optical anisotropy measurements show that aggregated NR assemblies are more anisotropic compared to isolated NRs and, therefore, provide an enhanced electrooptic response. A key insight from our study is that the fielddriven relative change in absorbance depends not only on the degree of NR alignment but also on the optical anisotropy of the absorbing species—that is, isolated NRs or NR assemblies. By analyzing our measurements using an optical model that we derived, we have quantified the degree of order in terms of the average emitter orientation relative to the field axis. Our results show a consistent improvement in macroscopic alignment as a function of NR concentration, with a minimum average deviation angle of 36.2° based on our extrapolated values for anisotropy. Our results also indicate that NR bundles are more responsive to field-driven alignment compared to individual NRs. This work provides a fundamental basis for quantifying the AC field-driven ordering of colloidal NRs and may further aid the design of optoelectronic devices with aligned anisotropic nanocrystals.

METHODS

Materials. Cadmium oxide (CdO, ≥99.99% trace metals basis), selenium (99.99% trace metals basis), sulfur (99.998% trace metals basis), octadecylphosphonic acid (ODPA, 97%), hexylphosphonic acid (95%), trioctylphosphine oxide (TOPO, ReagentPlus, 99%), trioctylphosphine (TOP, 97%), 1-octadecene (ODE, technical grade 90%), hexanes (anhydrous mixture of isomers, 99%), and methanol (anhydrous, 99.8%) were purchased from Sigma-Aldrich.

Preparation of CdSe/CdS NRs. Colloidal CdSe/CdS NRs were synthesized using a seeded growth method previously described by Carbone et al. 35 The as-synthesized nanorods were precipitated with the addition of methanol as an antisolvent and purified by centrifugation at 3000 rcf for 8 min. The resulting precipitate was further cleaned by being resuspended in a mixture of hexane and methanol followed by centrifugation at 3000 rcf for 8 min. This purification step was repeated twice before the final precipitate was resuspended in 10 mL of anhydrous hexane and stored under argon for further analysis.

Characterization. High-resolution transmission electron microscopy (HR-TEM) images were collected using an FEI Tecnai G2 F20 ST FE-TEM operated at an accelerating voltage of 200 kV. Absorbance and PL spectra were collected on an Ocean Optics Flame-S UV-vis spectrometer with an Ocean Optics DH-2000-BAL deuterium and halogen lamp as the light source. Powder XRD measurements were performed using a Bruker-AXS D8 Advanced Bragg-Brentano diffractometer with a Cu K α radiation source (λ = 1.5418 Å).

Optical Response Measurements. Sinusoidal AC electric fields were applied across colloidal dispersions of CdSe/CdS NRs using a function generator (RIGOL DG1032) coupled with a high-voltage amplifier (Trek model 2220). Concurrent changes in optical transmission of a 405 nm laser (RGBLase FBB-405-200-FS-C-1-0) were measured using a photoreceiver (2007 Nirvana auto-balanced optical receiver) and a digital oscilloscope (RIGOL DS2302A). Sample cells were prepared by adhering pairs of patterned ITO glass slides (MSE Supplies) using a mixture of optical adhesive (Norland NOE81) and 50 μ m spacer beads (Cospheric). Detailed schematics of the experimental setup and sample cell design are included in the Supporting Information.

Fluorescence Anisotropy Measurements. Conventional and circular-polarized ensemble fluorescence anisotropy measurements were carried out using a home-built L-format optical setup (see Figure S6 in Supporting Information) equipped with a 405 nm laser (RGBLase FBB-405-200-FS-C-1-0). The excitation beam was attenuated using a variable neutral density filter (Thorlabs NDC-25C-2) and polarized through a hand-mounted Glan-Taylor polarizer (Thorlabs GT15-A). A zero-order quarter-wave plate (Thorlabs WPQ05M-405) mounted on a high-precision rotation mount (Thorlabs PRM1) was used to achieve circular-polarized excitation. The PL emission from the sample was collected at 90° relative to the excitation beam using coaligned irises (Thorlabs ID25) and polarized using a second Glan-Taylor polarizer (Thorlabs GT15-A) before being directed to a free-space biased Si photodetector (Thorlabs DET100A2).

ASSOCIATED CONTENT

5 Supporting Information

The Supporting Information is available free of charge at https://pubs.acs.org/doi/10.1021/acsnano.1c08488.

TEM images and XRD pattern; schematics describing experimental setups for measuring time-dependent absorbance and ensemble fluorescence anisotropy; additional optical response and ensemble anisotropy data measured using an alternate batch of CdSe/CdS NRs; SAXS patterns of CdSe/CdS NR colloids; plot of average deviation angle vs. focus factor (κ); derivation of theoretical expressions for vertical- and circular-polarized ensemble fluorescence anisotropy (PDF)

AUTHOR INFORMATION

Corresponding Author

Matthew T. Sheldon – Department of Chemistry, Texas A&M University, College Station, Texas 77843-3255, United States; Department of Materials Science & Engineering, Texas A&M University, College Station, Texas 77843-3255, *United States;* © orcid.org/0000-0002-4940-7966; Email: sheldonm@tamu.edu

Authors

Rivi J. Ratnaweera – Department of Chemistry, Texas A&M University, College Station, Texas 77843-3255, United States; orcid.org/0000-0001-7343-5695

Freddy A. Rodríguez Ortiz – Department of Chemistry, Texas A&M University, College Station, Texas 77843-3255, United States; orcid.org/0000-0001-8289-2281

Nicholas J. Gripp – Department of Materials Science & Engineering, Texas A&M University, College Station, Texas 77843-3255, United States

Complete contact information is available at: https://pubs.acs.org/10.1021/acsnano.1c08488

Author Contributions

M.T.S. and R.J.R. conceived the idea. R.J.R., F.A.R.O., and N.J.G. designed and conducted the experiments. R.J.R. and F.A.R.O. performed characterization. R.J.R. derived the theoretical equations. R.J.R., F.A.R.O., and M.T.S. wrote the manuscript. All authors reviewed the manuscript.

The authors declare no competing financial interest. A preprint of the manuscript is available through the ChemRxiv repository: Ratnaweera, R.; Rodríguez Ortiz, F.; Gripp, N.; Sheldon, M. Quantifying Order during Field-Driven Alignment of Colloidal Semiconductor Nanorods. *ChemRxiv* 2021, 10.26434/chemrxiv-2021-dllkj.

ACKNOWLEDGMENTS

This work was supported by the Gordon and Betty Moore Foundation (Grant No. GBMF6882), the Welch Foundation (A-1886), the Air Force Office of Scientific Research (FA9550-16-1-0154), and the National Science Foundation (Grant No. DMR-2131408). The authors would like to thank Je-Ruei Wen for assistance with TEM imaging as well as Ryan Kutayiah and Benjamin Roman for invaluable discussion.

REFERENCES

- (1) Bronstein, N. D.; Li, L.; Xu, L.; Yao, Y.; Ferry, V. E.; Alivisatos, A. P.; Nuzzo, R. G. Luminescent Solar Concentration with Semiconductor Nanorods and Transfer-Printed Micro-Silicon Solar Cells. *ACS Nano* **2014**, *8*, 44–53.
- (2) Cunningham, P. D.; Souza, J. B.; Fedin, I.; She, C.; Lee, B.; Talapin, D. V. Assessment of Anisotropic Semiconductor Nanorod and Nanoplatelet Heterostructures with Polarized Emission for Liquid Crystal Display Technology. *ACS Nano* **2016**, *10*, 5769–5781.
- (3) Deka, S.; Quarta, A.; Lupo, M. G.; Falqui, A.; Boninelli, S.; Giannini, C.; Morello, G.; De Giorgi, M.; Lanzani, G.; Spinella, C.; Cingolani, R.; Pellegrino, T.; Manna, L. CdSe/CdS/ZnS Double Shell Nanorods with High Photoluminescence Efficiency and Their Exploitation As Biolabeling Probes. J. Am. Chem. Soc. 2009, 131, 2948–2958.
- (4) Fisher, M.; Farrell, D.; Zanella, M.; Lupi, A.; Stavrinou, P. N.; Chatten, A. J. Utilizing Vertically Aligned CdSe/CdS Nanorods Within a Luminescent Solar Concentrator. *Appl. Phys. Lett.* **2015**, *106*, 041110.
- (5) Martin, J.; Ratnaweera, R.; Kumar, S.; Wen, J.-R.; Kutayiah, A. R.; Sheldon, M. Detailed Balance Efficiencies for Luminescent Solar Concentrators with Aligned Semiconductor Nanorods: the Benefits of Anisotropic Emission. *J. Photonics Energy* **2020**, *10*, 025501.
- (6) Pisanello, F.; Martiradonna, L.; Spinicelli, P.; Fiore, A.; Hermier, J. P.; Manna, L.; Cingolani, R.; Giacobino, E.; De Vittorio, M.; Bramati, A. Dots in Rods As Polarized Single Photon Sources. *Superlattices Microstruct.* **2010**, *47*, 165–169.
- (7) Rizzo, A.; Nobile, C.; Mazzeo, M.; De Giorgi, M.; Fiore, A.; Carbone, L.; Cingolani, R.; Manna, L.; Gigli, G. Polarized Light Emitting Diode by Long-Range Nanorod Self-Assembling on a Water Surface. *ACS Nano* **2009**, *3*, 1506–1512.
- (8) Coropceanu, I.; Rossinelli, A.; Caram, J. R.; Freyria, F. S.; Bawendi, M. G. Slow-Injection Growth of Seeded CdSe/CdS Nanorods with Unity Fluorescence Quantum Yield and Complete Shell to Core Energy Transfer. ACS Nano 2016, 10, 3295–3301.
- (9) Diroll, B. T.; Dadosh, T.; Koschitzky, A.; Goldman, Y. E.; Murray, C. B. Interpreting the Energy-Dependent Anisotropy of Colloidal Nanorods Using Ensemble and Single-Particle Spectroscopy. *J. Phys. Chem. C* 2013, *117*, 23928–23937.
- (10) Diroll, B. T.; Koschitzky, A.; Murray, C. B. Tunable Optical Anisotropy of Seeded CdSe/CdS Nanorods. *J. Phys. Chem. Lett.* **2014**, *5*, 85–91.
- (11) Hadar, I.; Hitin, G. B.; Sitt, A.; Faust, A.; Banin, U. Polarization Properties of Semiconductor Nanorod Heterostructures: From Single Particles to the Ensemble. *J. Phys. Chem. Lett.* **2013**, *4*, 502–507.
- (12) Krahne, R.; Morello, G.; Figuerola, A.; George, C.; Deka, S.; Manna, L. Physical Properties of Elongated Inorganic Nanoparticles. *Phys. Rep.* **2011**, *501*, 75–221.
- (13) Jing, L.; Kershaw, S. V.; Li, Y.; Huang, X.; Li, Y.; Rogach, A. L.; Gao, M. Aqueous Based Semiconductor Nanocrystals. *Chem. Rev.* **2016**, *116*, 10623–10730.
- (14) Ussembayev, Y. Y.; Hens, Z.; Neyts, K. Contrasting Anisotropy of Light Absorption and Emission by Semiconductor Nanoparticles. *ACS Photonics* **2019**, *6*, 1146–1152.

- (15) Verbunt, P. P. C.; de Jong, T. M.; de Boer, D. K. G.; Broer, D. J.; Debije, M. G. Anisotropic Light Emission from Aligned Luminophores. *Eur. Phys. J. Appl. Phys.* **2014**, *67*, 10201.
- (16) Li, L.-S.; Alivisatos, A. P. Semiconductor Nanorod Liquid Crystals and Their Assembly on a Substrate. *Adv. Mater.* **2003**, *15*, 408–411.
- (17) Li, L.-s.; Walda, J.; Manna, L.; Alivisatos, A. P. Semiconductor Nanorod Liquid Crystals. *Nano Lett.* **2002**, *2*, 557–560.
- (18) Vanmaekelbergh, D. Self-Assembly of Colloidal Nanocrystals As Route to Novel Classes of Nanostructured Materials. *Nano Today* **2011**, *6*, 419–437.
- (19) Kutayiah, A. R.; Kumar, S.; Ratnaweera, R.; Easwaran, K.; Sheldon, M. Markov Chains for Modeling Complex Luminescence, Absorption, and Scattering in Nanophotonic Systems. *Opt. Express* **2021**, *29*, 4249–4269.
- (20) Ramasamy, K.; Gupta, A. Routes to Self-Assembly of Nanorods. *J. Mater. Res.* **2013**, 28, 1761–1776.
- (21) Baker, J. L.; Widmer-Cooper, A.; Toney, M. F.; Geissler, P. L.; Alivisatos, A. P. Device-Scale Perpendicular Alignment of Colloidal Nanorods. *Nano Lett.* **2010**, *10*, 195–201.
- (22) Querner, C.; Fischbein, M. D.; Heiney, P. A.; Drndić, M. Millimeter-Scale Assembly of CdSe Nanorods into Smectic Super-structures by Solvent Drying Kinetics. *Adv. Mater.* **2008**, *20*, 2308–2314.
- (23) Talapin, D. V.; Shevchenko, E. V.; Murray, C. B.; Kornowski, A.; Förster, S.; Weller, H. CdSe and CdSe/CdS Nanorod Solids. *J. Am. Chem. Soc.* **2004**, *126*, 12984–12988.
- (24) Zanella, M.; Gomes, R.; Povia, M.; Giannini, C.; Zhang, Y.; Riskin, A.; Van Bael, M.; Hens, Z.; Manna, L. Self-Assembled Multilayers of Vertically Aligned Semiconductor Nanorods on Device-Scale Areas. *Adv. Mater.* **2011**, *23*, 2205–2209.
- (25) Amit, Y.; Faust, A.; Lieberman, I.; Yedidya, L.; Banin, U. Semiconductor Nanorod Layers Aligned Through Mechanical Rubbing. *Phys. Status Solidi A* **2012**, 209, 235–242.
- (26) Hu, Z.; Fischbein, M. D.; Querner, C.; Drndić, M. Electric-Field-Driven Accumulation and Alignment of CdSe and CdTe Nanorods in Nanoscale Devices. *Nano Lett.* **2006**, *6*, 2585–2591.
- (27) Mohammadimasoudi, M.; Hens, Z.; Neyts, K. Full Alignment of Dispersed Colloidal Nanorods by Alternating Electric Fields. *RSC Adv.* **2016**, *6*, 55736–55744.
- (28) Fukagawa, T.; Tajima, R.; Yamaguchi, Y.; Tanaka, H.; Morikawa, K.; Tanaka, S.; Hatakeyama, Y.; Hino, K. Effect of an External DC Electric Field on the Order of Polymer-Capped Gold Nanorods: Formation of Smectic, Tetragonal, and Hexagonal Structures. *J. Phys. Chem. C* **2021**, *125*, 11085–11096.
- (29) Zhang, H.; Liu, Y.; Shahidan, M. F. S.; Kinnear, C.; Maasoumi, F.; Cadusch, J.; Akinoglu, E. M.; James, T. D.; Widmer-Cooper, A.; Roberts, A.; Mulvaney, P. Direct Assembly of Vertically Oriented, Gold Nanorod Arrays. *Adv. Funct. Mater.* **2021**, *31*, 2006753.
- (30) Pietra, F.; Rabouw, F. T.; van Rhee, P. G.; van Rijssel, J.; Petukhov, A. V.; Erné, B. H.; Christianen, P. C. M.; de Mello Donegá, C.; Vanmaekelbergh, D. Self-Assembled CdSe/CdS Nanorod Sheets Studied in the Bulk Suspension by Magnetic Alignment. *ACS Nano* **2014**, *8*, 10486–10495.
- (31) Kamal, J. S.; Gomes, R.; Hens, Z.; Karvar, M.; Neyts, K.; Compernolle, S.; Vanhaecke, F. Direct Determination of Absorption Anisotropy in Colloidal Quantum Rods. *Phys. Rev. B* **2012**, *85*, 035126.
- (32) Nann, T.; Schneider, J. Origin of Permanent Electric Dipole Moments in Wurtzite Nanocrystals. *Chem. Phys. Lett.* **2004**, 384, 150–152.
- (33) Rossi, D.; Han, J. H.; Jung, W.; Cheon, J.; Son, D. H. Orientational Control of Colloidal 2D-Layered Transition Metal Dichalcogenide Nanodiscs *via* Unusual Electrokinetic Response. *ACS Nano* **2015**, *9*, 8037–8043.
- (34) Mardia, K. V.; Jupp, P. E. Tests on von Mises Distributions. *Directional Statistics*; John Wiley & Sons, Inc.: Hoboken, NJ, 1999; pp 119–142.

- (35) Carbone, L.; Nobile, C.; De Giorgi, M.; Sala, F. D.; Morello, G.; Pompa, P.; Hytch, M.; Snoeck, E.; Fiore, A.; Franchini, I. R.; Nadasan, M.; Silvestre, A. F.; Chiodo, L.; Kudera, S.; Cingolani, R.; Krahne, R.; Manna, L. Synthesis and Micrometer-Scale Assembly of Colloidal CdSe/CdS Nanorods Prepared by a Seeded Growth Approach. *Nano Lett.* **2007**, *7*, 2942–2950.
- (36) Ameloot, M.; vandeVen, M.; Acuña, A. U.; Valeur, B. Fluorescence Anisotropy Measurements in Solution: Methods and Reference Materials (IUPAC Technical Report). *Pure Appl. Chem.* **2013**, *85*, 589–608.
- (37) Lakowicz, J. R. Fluorescence Anisotropy. *Principles of Fluorescence Spectroscopy*, 3rd ed.; Springer: Boston, MA, 2006; pp 291–319.
- (38) Skoog, D. A.; West, D. M.; Holler, F. J.; Crouch, S. R. Spectrochemical Methods. *Fundamentals of Analytical Chemistry*, 9th ed.; Cengage Learning: Belmont, CA, 2013; pp 649–817.

□ Recommended by ACS

Liquid Crystal Films as Active Substrates for Nanoparticle Control

Ines Gharbi, Emmanuelle Lacaze, et al.

JUNE 21, 2021

ACS APPLIED NANO MATERIALS

READ 🗹

Toward Huygens' Sources with Dodecahedral Plasmonic Clusters

Laurent Lermusiaux, Alexandre Baron, et al.

FEBRUARY 18, 2021

NANO LETTERS

READ 🗹

Light-Induced Coalescence of Plasmonic Dimers and Clusters

Andrew R. Salmon, Jeremy J. Baumberg, et al.

MARCH 25, 2020

ACS NANO

READ 🗹

Identification of Brillouin Zones by In-Plane Lasing from Light-Cone Surface Lattice Resonances

Jun Guan, Teri W. Odom, et al.

MARCH 09, 2021

ACS NANO

READ Z

Get More Suggestions >